An Example of Principal Component Analysis Applied to Correlated Images

Anthony A. Maciejewski
Dept. of Electrical & Computer Engineering
Purdue University,
1285 Electrical Engineering Bldg.,
West Lafayette, IN 47907-1285 USA

Rodney G. Roberts
Dept. of Electrical & Computer Engineering
FAMU-FSU College of Engineering
2525 Pottsdamer Street
Tallahassee, FL 32310-6046 USA

Abstract—**The use of Principal Component Analysis (PCA), also known as Singular Value Decomposition (SVD), is a powerful tool that is frequently applied to the classification of hyperspectral images in remote sensing. Unfortunately, the utility of the resulting PCA may depend on the resolution of the original image, i.e., too coarse-grained of an image may result in inaccurate major principal components. This work presents an example of how the major principal component obtained from the PCA of a low-resolution image may be refined to obtain a more accurate estimate of the major principal component. The more accurate estimate is obtained by recursively performing a PCA on only those pixels that contribute strongly to the major principal component.**

I. INTRODUCTION

Image analyses inherently require the handling of large volumes of information so that efficient mechanisms are required for the organization and classification of image data. One common reduced order representation for images, especially images that consist of multidimensional data, is based on the singular value decomposition (SVD). Variously referred to as eigendecomposition, principal component analysis (PCA) and Karhunen-Loeve transformation [1], the SVD has been successfully applied to a variety of imaging problems including face characterization [2] and recognition [3], lip-reading [4, 5], robot vision [6], video analysis [7], and remote sensing [8-10]. All of these applications are based on taking advantage of the fact that a set of highly correlated images can be approximately represented by a small set of singular vectors.

In this work, we consider the application of remote sensing; in particular, the analysis of hyperspectral images where there is multidimensional data (the spectral reflectance at various different wavelengths) associated with every pixel in an image. While PCA is commonly used in the representation and classification of such images, the singular vectors resulting from the analysis depend on the resolution of the original image. In general, the singular vectors obtained from higher-resolution images are more useful than those from lower-resolution images. We illustrate a technique by which the singular vector associated with the maximum singular value for a high-resolution hyperspectral image can be approximated from a lower-resolution image. An overview of PCA for hyperspectral images along with our proposed technique is presented in the following section. Section III presents an example of applying our approach to a specific hyperspectral image. Finally, the conclusions of this work are presented in Section IV.

II. APPROACH

Let f_i represent an m-dimensional vector that corresponds to the spectral reflectance at pixel i. A hyperspectral image can then be represented by the matrix $F = [f_1, \ldots, f_n]$ where n is the total number of pixels in the image. Let the SVD of F be

$$F = U \Sigma V^T$$

where U and V are orthogonal, and Σ is a matrix with nonzero terms appearing only on the main diagonal, and in descending order. The columns of U, denoted u_i, are referred to as the left singular vectors of F; these provide an orthonormal basis for the spectral reflectance, ordered in terms of importance. The corresponding singular values, which are nonnegative, measure how "aligned" the spectral signatures of the pixels are with the associated left singular vector. Thus, the first left singular vector can be interpreted as the spectral signature containing the "most common" information from all of the pixels in the image. Likewise, the first k left singular vectors provide a basis for the best k-dimensional representation of the spectral response for the entire image. Thus the SVD provides a natural, ordered hierarchy for the compressed representation of information to within a user-defined level of accuracy. In addition to the left singular vectors, the information contained in the vectors comprising V (referred to as the right singular vectors and denoted v_i) also provide useful information for analyzing hyperspectral images. Specifically, the components of v_i measure how much each individual pixel contributes to the spectral signature represented by u_i.

Now consider a lower-resolution version of the hyperspectral image F, denoted by F'. Let the images F and F' represent the same total area, but with a pixel in F' being

0-7803-6661-1/01/$10.00 ©2001 IEEE

four times the area of a pixel in F. The lower resolution image can then be approximately represented by

$$F' = F\,G$$

where G is an n by $n/4$ matrix whose ith column is a vector containing all zeros except for the four entries in the $4(i\text{-}1)+1$ to the $4(i\text{-}1)+4$ location which contain 1/4. In other words, each pixel f_i' in the lower-resolution image is the average of four neighboring pixels in the higher-resolution image. Clearly, the SVD of F' will be different from that of F, which is arguably more useful because it represents more information. The question considered here is: Can one estimate the SVD of F when only F' is available?

To estimate the most significant spectral signature in F, i.e., the vector u_1, we use the following approach: First we calculate the SVD of the complete low-resolution image F'. We then examine the resulting maximum left singular v_1 and identify those elements, i.e., pixels, that have the largest value. We then construct a new matrix consisting of only these pixels and then compute its SVD. This process is then repeated until the resulting maximum left singular vector has converged or until a minimum number of pixels has been selected. Intuitively, one can expect this procedure to converge to a reasonable approximation of u_1 if those pixels that have a large component in v'_1 come from areas in the image that are relatively homogeneous and have a strong contribution to v_1. The following section presents an example of such a case.

III. RESULTS

The hyperspectral image used in this study was produced by the MODIS/ASTER (MASTER) sensor during flight #99-005-06 on June 3, 1999 over Albuquerque and Sevilleta, NM [11]. The sensor produces a 50-band image covering the spectrum from 0.4-13 micrometers. The spectral characteristics of the sensor are given in Table 1. This investigation focused on classification of the groundcover in an area near Ballenger Ranch, south of Edgewood, NM. This area was manually classified using aerial photographs and ground surveys into two main groups, i.e., either dominated by woodland or dominated by grasses. These categories were further subcategorized as either heavy or light woodland (classes 1 and 2 respectively) or pinon-juniper savanna, shrub, or grassland (classes 3, 4, and 5 respectively). This classification is shown in Fig. 1 with statistics presented in Table 2.

A principal component analysis was performed on a 20-meter resolution version of the MASTER image that was registered to correspond to the classified image in Fig. 1. The first two most significant spectral signatures, i.e., the left singular vectors associated with the two largest singular values, are shown in Fig. 2. A scatter plot of the pixels from the MASTER image projected on to these first two principal components is given in Fig. 3. From this scatter plot, it is clear that the value of the projection onto the first principal component is a good indicator of the type of groundcover, i.e., a large value indicates grassland whereas a small value indicates woodland. Indeed, the spectral response of the principal left singular vector is dominated by those pixels that represent grassland. This can be clearly seen by comparing Fig. 4, which is a plot of the right singular vector associated with the maximum singular value, with the classified image in Fig. 1.

TABLE 1
SPECTRAL CHARACTERISTICS OF THE MASTER SENSOR

BAND	HALFPP	HALFPP	FWHM	CENTER	PEAK
01	0.4373	0.4812	0.0439	0.4592	0.4600
02	0.4786	0.5213	0.0427	0.5000	0.5000
03	0.5202	0.5628	0.0426	0.5415	0.5420
04	0.5616	0.6026	0.0409	0.5821	0.5820
05	0.6320	0.6913	0.0593	0.6616	0.6540
06	0.6916	0.7333	0.0416	0.7125	0.7120
07	0.7307	0.7728	0.0421	0.7517	0.7520
08	0.7810	0.8233	0.0423	0.8021	0.8020
09	0.8486	0.8907	0.0421	0.8697	0.8700
10	0.8862	0.9271	0.0408	0.9066	0.9080
11	0.9260	0.9665	0.0404	0.9462	0.9480
12	1.5876	1.6418	0.0542	1.6147	1.6140
13	1.6432	1.6981	0.0549	1.6707	1.6700
14	1.6984	1.7515	0.0532	1.7249	1.7240
15	1.7520	1.8075	0.0555	1.7797	1.7800
16	1.8061	1.8593	0.0531	1.8327	1.8320
17	1.8558	1.9101	0.0543	1.8830	1.8780
18	1.9059	1.9613	0.0554	1.9336	1.9340
19	1.9555	2.0096	0.0541	1.9825	1.9820
20	2.0583	2.1118	0.0535	2.0851	2.0860
21	2.1381	2.1916	0.0536	2.1649	2.1660
22	2.1873	2.2422	0.0549	2.2147	2.2160
23	2.2375	2.2903	0.0528	2.2639	2.2640
24	2.2975	2.3677	0.0701	2.3326	2.3280
25	2.3664	2.4317	0.0653	2.3990	2.3960
26	3.0472	3.2041	0.1570	3.1257	3.1200
27	3.2081	3.3548	0.1467	3.2815	3.2750
28	3.3552	3.5119	0.1567	3.4336	3.4400
29	3.5138	3.6683	0.1546	3.5911	3.5900
30	3.6702	3.8093	0.1392	3.7398	3.7400
31	3.8229	3.9769	0.1540	3.8999	3.9000
32	3.9806	4.1324	0.1518	4.0565	4.0550
33	4.1351	4.2880	0.1530	4.2116	4.2070
34	4.2851	4.4380	0.1530	4.3616	4.3570
35	4.4465	4.5911	0.1446	4.5188	4.5200
36	4.5915	4.7478	0.1563	4.6696	4.6700
37	4.7494	4.9002	0.1508	4.8248	4.8250
38	4.9042	5.0464	0.1422	4.9753	4.9750
39	5.0481	5.2026	0.1544	5.1254	5.1250
40	5.2046	5.3425	0.1379	5.2735	5.2750
41	7.5724	7.9247	0.3523	7.7485	7.7926
42	7.9271	8.3734	0.4463	8.1502	8.2048
43	8.4203	8.7868	0.3665	8.6035	8.6247
44	8.8268	9.2632	0.4363	9.0450	9.0543
45	9.4762	9.8705	0.3942	9.6734	9.6654
46	9.8933	10.2792	0.3859	10.0862	10.0845
47	10.3130	10.9138	0.6009	10.6134	10.5542
48	10.9570	11.6501	0.6931	11.3035	11.1838
49	11.8480	12.3429	0.4949	12.0955	12.0740
50	12.6152	13.1012	0.4861	12.8582	12.8455

Figure 1 Classification of groundcover near Ballenger Ranch (south of Edgewood, NM). Darker shades of gray represent heavier groundcover.

TABLE 2
CLASSIFICATION HISTOGRAM

Class	Area (number pixels)	%
1 Heavy Woodland	20,152	31.6%
2 Light Woodland	10,876	17.1%
Total Woodland (1 & 2)	31,028	48.7%
3 Pinon-Juniper Savanna	21,651	34.0%
4 Shrubs	4,220	6.6%
5 Grasses	6,866	10.8%
Total Grassland (3, 4, & 5)	32,737	51.3%

Unfortunately, if this same procedure is performed on a MASTER image of lower resolution, the maximum spectral signature may not be as significantly dominated by the pixels primarily associated with grassland, and thus will not be as useful for classification. To illustrate this point, a principal component analysis was performed on an 80-meter resolution MASTER image. The first three left singular vectors associated with the three largest singular values are plotted in Fig. 5. Note that the spectral characteristics of the first principal component differ significantly from those of the 20-meter case (see Fig. 2). In particular, there are now peaks at bands 17, 26, and 34 that were not previously present and the sharp drop between bands 41 and 42 is no longer apparent. While there are still many predominantly grassland pixels that contribute to this first singular vector (see Fig. 6), there is also a significant contribution by pixels that are a mixture of woodland and grassland. Thus to recover the spectral signature of a predominantly grassland groundcover, one must use a linear combination of all three of the most significant left singular vectors. This is particularly

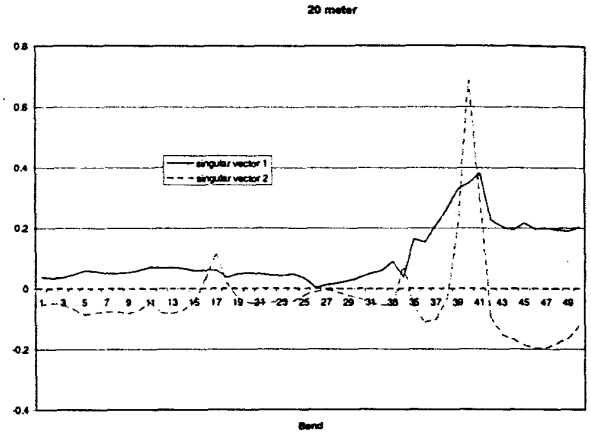

Figure 2 The two most significant spectral signatures, i.e., the singular vectors associated with the two largest singular values, for the 20-meter resolution MASTER image.

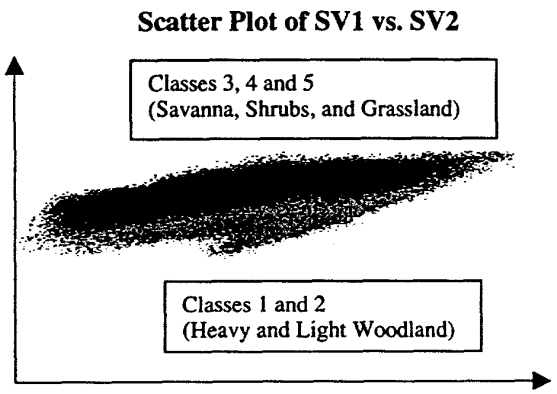

Figure 3 A scatter plot showing the projection of the 20-meter MASTER image onto the first two principal components.

noticeable by observing the strong negative peaks at bands 17, 26, and 34 of left singular vector three in Fig. 5. The fact that left singular vector 3 plays a much larger role in determining the spectral signature of grassland in the low resolution PCA can be verified by comparing the right singular vectors for both the 20-meter case and the 80-meter case, shown in Figs. 7 and 8, respectively.

Clearly, the principal components of the low-resolution image are affected by having a much larger number of pixels that consist of mixed ground cover. To see if the maximum principal component obtained from the higher resolution PCA could be obtained by only using the lower resolution image, the procedure outlined in the previous section was performed. In particular, the pixels that had the largest contribution to the first principal component were extracted from the image. This corresponds to the top 10% of the brightest pixels in Fig. 6. A new PCA was performed on only these pixels. This recursive application of the PCA to selected regions of the

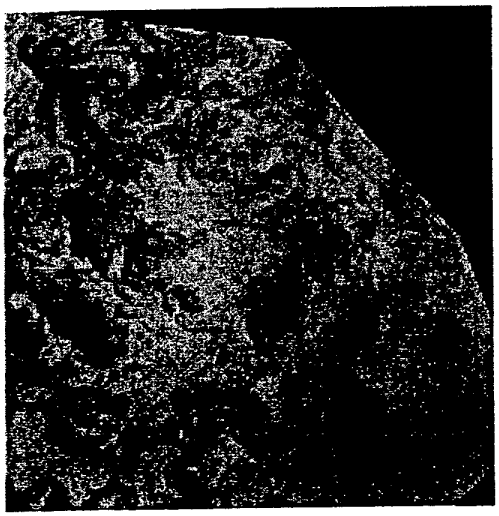

Figure 4 The right singular vector associated with the maximum singular value for the 20-meter resolution MASTER image. The light regions indicate a strong contribution to the maximum left singular vector and by comparison to Fig. 1 clearly correspond to regions associated with grassland groundcover.

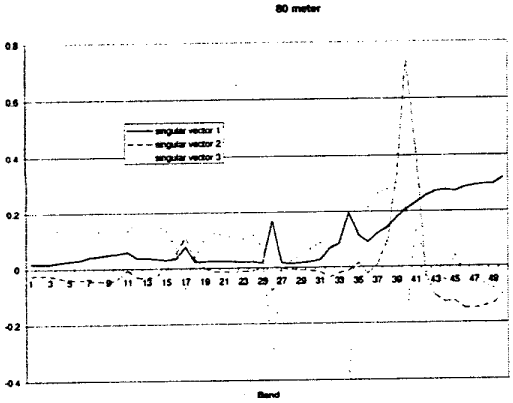

Figure 5 The three most significant spectral signatures, i.e., the singular vectors associated with the three largest singular values, for the 80-meter resolution MASTER image

image resulted in an increased contribution by pixels that were dominated by grassland. The resulting maximum left singular vector is shown in Fig. 9 and is very similar in spectral characteristics to the corresponding singular vector in the 20-meter case shown in Fig. 2. It is clearly superior to the maximum singular vector obtained from the initial PCA performed on the entire 80-meter image (shown in Fig. 5).

Figure 6 The right singular vector associated with the maximum singular value for the 80-meter resolution MASTER image. There is clearly a much larger contribution from areas that are not dominated by grassland as compared to the 20-meter case in Fig. 4.

IV. CONCLUSIONS

This work has presented an example of a case where the left singular vector associated with the maximum singular value, obtained by performing a principal component analysis on a low resolution hyperspectral image, can be refined to approach the value obtained if one had a much higher resolution image. This is useful because the singular vector associated with a higher resolution image more accurately reflects the spectral characteristics of the most dominant feature in the image and is thus more useful for classification. The more accurate estimate of the maximum singular vector is obtained by recursively performing a PCA on selected portions of the low-resolution image. It has *not* been shown that this procedure always results in a more accurate estimate. Also, it may be possible to extend this procedure to obtain estimates of all significant singular vectors, in addition to the one associated with the maximum singular value. Both of these points are the subjects of our current work.

V. ACKNOWLEDGMENTS

This work was supported by the National Imagery and Mapping Agency under contract no. NMA201-00-1-1003. The authors gratefully acknowledge the assistance of Paul Neville and Sandra White of the Earth Data Analysis Center, The University of New Mexico, for providing the authors with the images and data for this work. The authors would also like to thank Dave Landgrebe and Larry Biehl of Purdue University for providing the MultiSpec data analysis software system that was used in much of the analysis. (The MultiSpec software and documentation is available at http://dynamo.ecn.purdue.edu/~biehl/MultiSpec)

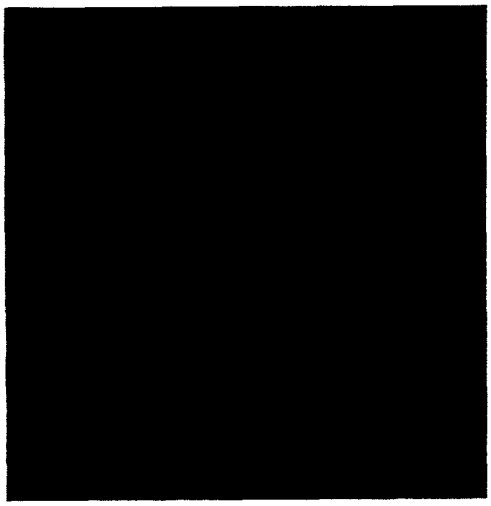

Figure 7 The right singular vector associated with the third largest singular value for the 20-meter resolution MASTER image. Note that there is very little contribution of the associated left singular vector.

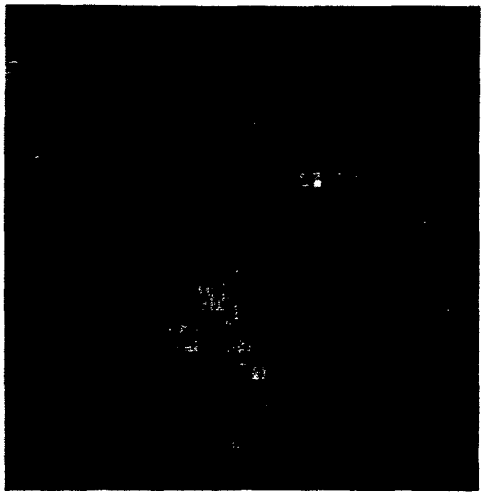

Figure 8 The right singular vector associated with the third largest singular value for the 80-meter resolution MASTER image. Note that there is significantly more contribution of the associated left singular vector than with that of the 20-meter image shown in Fig. 7.

VI. REFERENCES

[1] K. Fukunaga, *Introduction to statistical pattern recognition*, Academic Press, London, second edition, 1990.

[2] L. Sirovich and M. Kirby, "Low-dimensional procedure for the characterization of human faces," *Journal of Optical Society of America*, vol. 4, no. 3, pp. 519 -524, March 1987.

[3] M. Turk and A. Pentland, "Eigenfaces for recognition," *Journal of Cognitive Neuroscience*, vol. 3, no. 1, pp. 71 -86, March 1991.

[4] H. Murase and R. Sakai, "Moving object recognition in eigenspace representation: Gait analysis and lip reading," *Pattern Recognition Letters*, vol. 17, no. 2, pp. 155 -162, Feb. 1996.

[5] G. Chiou and J.-N. Hwang, "Lipreading from color video," *IEEE Transactions on Image Processing*, vol. 6, no. 8, pp. 1192 -1195, Aug. 1997.

[6] S. K. Nayar, S. A. Nene, and H. Murase, "Subspace method for robot vision," *IEEE Transactions on Robotics and Automation*, vol. 12, no. 5, Oct. 1996.

[7] K. J. Han and A. H. Tewfik, "Eigen-image based video segmentation and indexing," *Proc. IEEE International Conference on Image Processing.*, pp. 538 -541, (Alamitos, CA, USA), 1997.

[8] X. Jia and J. A. Richards, "Segmented principal components transformation for efficient hyperspectral remote-sensing image display and classification," *IEEE Trans. Geoscience and remote sensing*, vol. 37, no. 1, Jan. 1999, pp. 538-542.

[9] C-I. Chang, Q. Diu, T-L. Sun, and M.L.G. Althouse, "A joint band prioritization and band-decorrelation approach to band selection for hyperspectral image classification," *IEEE Trans. Geoscience and remote sensing*, vol. 37, no. 6, Nov. 1999, pp. 2631-2641.

[10] J. A. Richards and X. Jia, *Remote Sensing Digital Image Analysis*, Springer, NY 1999.

[11] http://masterweb.jpl.nasa.gov/

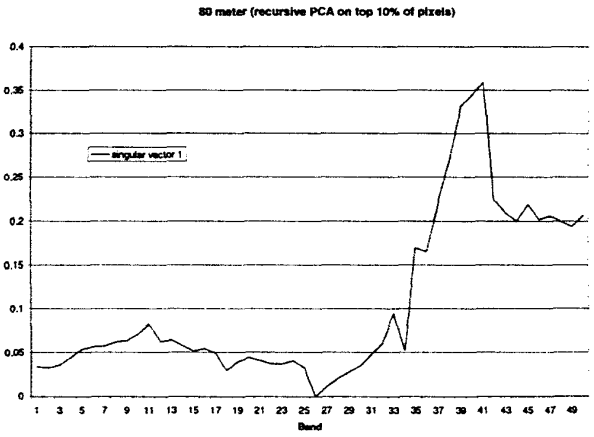

Figure 9 The left singular vector associated with the largest singular value for the 80 meter resolution MASTER image after recursively performing a PCA on the 10% of the pixels that had the highest contribution to this principal component. Note that the spectral characteristics of this maximum left singular vector are very similar to that of the higher resolution image given in Fig. 2.